Thin Solid Films 518 (2010) 7167–7173

Contents lists available at ScienceDirect

Thin Solid Films

journal homepage: www.elsevier.com/locate/tsf

Hydrogen absorption in epitaxial *bcc* V (001) thin films analysed by statistical thermodynamics

Nobumitsu Shohoji

LNEG — Laboratório Nacional de Energia e Geologia, LEN — Laboratório de Energia, Estrada do Paço do Lumiar, 22, 1649-038 Lisboa, Portugal

ARTICLE INFO

Article history:
Received 30 June 2009
Received in revised form 15 June 2010
Accepted 22 June 2010
Available online 30 June 2010

Keywords:
V–H
Epitaxial thin film
Non-stoichiometry
Interstitial solid solution
Statistical thermodynamics

ABSTRACT

Andersson, Aits and Hjörvarsson of Uppsala University measured hydrogen uptake in epitaxial *bcc* (body centred cubic) vanadium (V) (001) thin films of thickness, 50 nm and 100 nm, over temperature range between 443 K and 513 K. The reported equilibrium pressure–temperature–composition (*P–T–C*) relationships for the epitaxial *bcc* V (001) thin films showed appreciable extent of enhancement of H solubility compared with that for bulk *bcc* V. In this work, the reported equilibrium *P–T–C* relationships for the epitaxial *bcc* V(001) thin films by Andersson et al. were analysed in terms of statistical thermodynamics for H_2 gas partial pressure $p(H_2)$ up to 100 Pa and H/V mole atom ratio x in VH_x up to 1. The present analysis results showed that, up to $x = 0.75$, the state of H in the V lattice was comparable to that in bulk VH_x specimen but that, in the range of x higher than 0.75, state of H in the thin film with the constrained basal plane condition was evidently distinguishable from that in non-constrained bulk VH_x. This was concluded to be the consequence of the tetragonal distortion of the *bcc* lattice with biaxially constrained condition at the bottom surface of the VH_x (001) thin film in the range of x exceeding 0.75.

1. Introduction

Equilibrium H (hydrogen) absorption isotherms in epitaxial *bcc* (body centred cubic) vanadium (001) thin films with thickness, 50 nm and 100 nm, were determined resistometrically by Andersson et al. [1] over range of temperature T between 443 K and 513 K. The epitaxial *bcc* V (001) thin films were reported to be deposited over MgO (001) substrate by magnetron sputtering. The H/V atom ratio (x in VH_x) in the epitaxial VH_x (001) thin films reached to about 0.9 without any detectable phase transformation by raising the hydrogen gas partial pressure $p(H_2)$ up to 100 Pa. Thereafter, Olsson and Hjörvarsson presented further detailed analysis on the nature of the H–H interaction [2] and on the reversible structure change and the thermodynamic properties [3] in the epitaxial *bcc* VH_x (001) thin films. They concluded [2,3] that the H solubility in the biaxially constrained V thin film was sensitively affected by the stress state in the thin film. While the induced biaxial compressive stress to the *bcc* V (001) thin film led to the enhanced H solubility compared with that in the bulk V as reported by Andersson et al. [1], such stress might result in suppressed H solubility in some thin film as referred to for thin epitaxial Nb (110) film [3].

In a preceding work, Hjörvarsson et al. [4] demonstrated that thickness of interface region of very thin epitaxial V(110) film deposited over Mo substrate was about 4 ML (molecular layer). They also reported that H absorption in the 4 ML thick interface region of the V(110) thin film was substantially suppressed compared with that in the bulk V specimen reported earlier by Veleckis and Edwards [5]. Their experiments were done for the test pieces of V(110) thin films of the thickness between 6.1 ML (1.30 nm) and 3.5 ML (0.74 nm). They reported that there was no evidence of H uptake in the substrate Mo [4].

Thus, it must be of pragmatic significance to analyse H absorption performances for epitaxial metal thin films with varying growth orientations deposited over non-H absorbing substrate in terms of statistical thermodynamics to compare the H absorption performances in the epitaxial thin films with specified growth orientations with those in the corresponding bulk metal samples (powder or thin film) under non-constrained state for the purpose of evaluating influence of biaxial strain on pairwise nearest neighbour atomic interactions, E(H–H) and E(H–M), in MH_x.

Equilibrium *P–T–C* (pressure–temperature–composition) relationships for H absorption in V as well as for the other two Va-group transition metals, Nb and Ta, were measured by Veleckis and Edwards [5] over range of T between 518.6 K and 827 K up to $p(H_2) = 800$ Torr ($\approx$100 Pa) for thin foil test piece using Sieverts' method.

Hydrogen absorption performance in epitaxial *bcc* V (001) thin film with mechanically constrained condition deposited over non-H absorbing solid substrate MgO [1] was appreciably different from that in bulk V metal in non-constrained state like free thin foil or powder form [4] as reproduced in Fig. 1 in which representative isothermal *P–C* relationships for bulk V (thin foil in non-constrained condition) [5] and those for epitaxial *bcc* V (001) thin films [1] are compared. Although direct comparison of the isotherms between the bulk V and

E-mail address: nobumitsu.shohoji@ineti.pt.

0040-6090/$ – see front matter © 2010 Elsevier B.V. All rights reserved.
doi:10.1016/j.tsf.2010.06.052

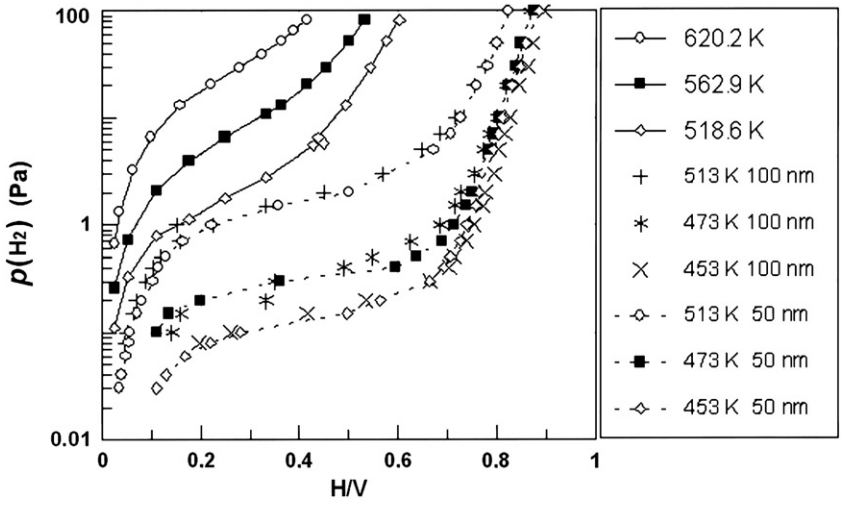

Fig. 1. Representative isothermal *P–C* plots for H absorption in 50 nm and 100 nm thick epitaxial *bcc* V (001) thin films reported by Andersson et al. [1] compared with those for H absorption in bulk V reported by Veleckis and Edwards [5]. 1 atm = 101.325 Pa.

the epitaxial *bcc* V (001) thin film at exactly identical *T* was not possible because the *T* range reported for the former was no lower than 518.6 K and that for the latter was no higher than 513 K, we see very clearly in Fig. 1 that H absorption in the epitaxial *bcc* V (001) thin film was enhanced compared with that in the bulk V under comparable conditions of $p(H_2)$ and *T*. For example, when compared at $p(H_2) = 10$ Pa, *x* in VH_x in the bulk test piece was no higher than 0.5 while that in the epitaxial *bcc* V (001) thin film exceeded 0.7.

Statistical thermodynamic analysis was made some years ago for H absorption in bulk V [6–10] using the *P–T–C* relationships reported by Veleckis and Edwards [5]. In the present work, statistical thermodynamic analysis is made for H absorption in the epitaxial *bcc* V (001) thin films to characterise the differences in H absorption performance between the epitaxial *bcc* V (001) thin film and the bulk V in terms of atomic interaction parameters evaluated by statistical thermodynamics. Further, influence of thickness of the epitaxial *bcc* V (001) thin film on the H absorption performance is reviewed.

2. Standard statistical thermodynamic analysis procedure

In the statistical thermodynamics, partition function *PF* for condensed phase (either solid or liquid) under consideration is composed taking into account pairwise nearest neighbour atomic interactions $E(i-j)$. Then, chemical potential $\mu(i)^c$ of the constituent element *i* in the condensed phase is derived through partial differentiation of *PF* with respect to the number n_i of the constituent element *i*. Subsequently, $\mu(i)^c$ in the condensed phase is put equal to $\mu(i)^g$ of the same element *i* in the gas phase.

The expression for $\mu(X)^g$ of ideal diatomic gas X_2 is readily available in the classical text book authored by Fowler and Guggenheim [11]. The detailed derivation procedure of $\mu(X)^c$ for the condensed phase MX_x might be referred to elsewhere [7–9]. The statistical thermodynamic equilibrium condition is eventually reduced to the following Eq. (1) for the purpose of analysing H solution under consideration

$$A(x,T) \equiv RT\ln\{[p(H_2)]^{1/2}\cdot(\theta-x)/x\} = g + \beta x E(\text{H–H}) \quad (1)$$

$$K = g-[D(H_2)/2-RTC(T)] = Q-RT\ln f_H(T) \quad (2)$$

$$C(T) = -(1/2)\ln\{[(4\pi m_H)^{3/2}k^{5/2}/h^3]\cdot[(T^{7/2}/\Theta_r)\cdot(1+\Theta_r/3T)] \times[\rho^2\upsilon_0^*/2]\} + \Theta_v/4T + (1/2)\ln[1-\exp(-\Theta_v/T)] \quad (3)$$

$$\ln f_H(T) = -\int_0^\infty g(\nu)\ln[1-\exp(-h\nu/kT)]d\nu + \ln\rho\upsilon_0 \quad (4)$$

$$Q + \beta x E(\text{H–H}) = \partial E/\partial n_H. \quad (5)$$

To start the statistical thermodynamic analysis using Eq. (1), the value for the parameter θ must be chosen adequately to yield linear $A(T)$ vs. *x* isotherms. This is to fulfil the *a priori* assumption of constant E(H–H) over a range of homogeneity composition *x* at a given *T* for VH_x.

In a preliminary statistical thermodynamic analysis of *P–T–C* relationships reported for H absorption for Va-group transition metals (V, Nb and Ta) by Veleckis and Edwards [5], it was demonstrated [6] that number θ of available interstitial sites for occupation by H atoms per metal atom was smaller than 1 whereas, in view of mere crystal geometry, θ is as high as 6 provided that T-sites (tetrahedral interstitial sites) are occupied with H atoms or $\theta = 3$ provided that O-sites (octahedral interstitial sites) are occupied with H atoms. The θ value determined was 0.75 for *bcc* NbH_x or 0.55 for *bcc* VH_x and for *bcc* TaH_x [6].

Such drastic reduction of number θ of really available site by interstitial atoms per metal atom in MX_x from the geometrically available number θ_0 of interstitial sites per metal atom in specified crystal structure ($\theta_0 = 6$ for T-sites and $\theta_0 = 3$ for O-sites in *bcc* lattice, as pointed out above) was proposed originally by Sepiser and Spretnak as early as 1955 [12]. This concept for non-stoichiometric interstitial solutions is known as "blocking" model. The results of available statistical thermodynamic analyses for a variety of M–H systems [6–10] appeared to imply that the "blocking effect leading to appreciably smaller θ than θ_0 must be the consequence of modification of electronic state in the MH_x lattice.

The determination of θ was made with an *a priori* assumption that the interaction energy E(H–H) between the nearest neighbour H atoms would hold constant within the same phase at a given *T* and the subsequent statistical thermodynamic analyses for a variety of non-stoichiometric interstitial MX_x systems (X = H, C, N, P or S but not O) were undertaken with this simplifying *a priori* assumption and the derived values for the interaction parameters $E(i-j)$ between neighbouring constituents *i* and *j* in the MX_x lattice appeared to be rational [6–10,13–16]. Thus, the employed *a priori* assumption for the series of statistical thermodynamic analyses was judged to be valid on the basis of the self-consistency of the evaluation results acquired by this simplifying postulate although there was no first-principle-based justification to validate this *a priori* assumption.

Noting that energy change involved even in the liquid/solid phase transition is a mere 10–20 kJ mol^{-1} [17], it is more natural and straightforward to accept that phase change is induced when considerable variation of E(X–X) with x in MX_x occurs at a given T.

3. *P–T–C* relationships for the *bcc* epitaxial VH_x (001) thin films

To carry out statistical thermodynamic analysis for the epitaxial *bcc* VH_x (001) thin films, it was desirable to convert the graphically presented *P–C* isotherms in Fig. 2 in Ref. [1] into numerical tables as summarised in Tables 1 and 2.

Table 1 summarises the numerical *P–T–C* data for the 100 nm film and Table 2 those for the 50 nm film. The *P–C* isotherms displayed in Fig. 1 were prepared from these data listed in Tables 1 and 2.

4. Determining the θ parameter value for the *bcc* epitaxial VH_x (001) thin film

To start statistical thermodynamic analysis for the epitaxial *bcc* VH_x thin films under consideration, the first step is to determine the value of θ.

In the earlier statistical thermodynamic analysis for bulk *bcc* VH_x [6] using *P–T–C* data reported by Veleckis and Edwards [5], θ was chosen to be 0.55 as well as for TaH_x while θ was chosen to be 0.75 for NbH_x [6]. However, it was felt inadequate to undertake the present analysis for H solution in the epitaxial V (001) thin film with the choice of $\theta = 0.55$ by looking at Fig. 1 that shows appreciable extent of H absorption enhancement in the epitaxial *bcc* V (001) thin film compared with that in the bulk V. Thence, with a tentative choice of $\theta = 1$, A vs. x plots for the 100 nm V film were prepared. Fig. 2 reproduces the prepared $A(T;\theta = 1)$ vs. x isotherms for 100 nm thick VH_x (001) film.

It is seen clearly in Fig. 2 that, at any examined T, slope of the A vs. x isotherm changes from negative to positive sharply with the rising x at around $x = 0.7$. The slope of A vs. x isotherm is proportional to the nearest neighbour H–H interaction energy E(H–H) as represented by Eq. (1). Thus, the trend demonstrated in Fig. 2 is considered to be compatible with the argument stated by Andersson et al. [1] claiming that E(H–H) turned from attractive (negative) to repulsive (positive) at around $x = 0.65$–0.7.

Table 1
P–T–C data for H absorption in the epitaxial *bcc* V (001) thin film of thickness 100 nm read from Fig. 2 in Ref. [1]. Bold letters refer to the compositions with H/V lower than 0.55. Shaded data points ($0.675 < x < 0.775$) in the intermediate H/V range were excluded from the analysis.

$p(H_2)$		H/V					
(atm)	**(Pa)**	513 K	498 K	483 K	473 K	463 K	453 K
1.0000	**101.325**	0.823	0.842	0.862	0.867	0.887	0.896
0.5000	**50.663**	0.800	0.817	0.834	0.849	0.862	0.873
0.3000	**30.398**	0.776	0.806	0.826	0.841	0.850	0.864
0.2000	**20.265**	0.754	0.782	0.805	0.818	0.830	0.845
0.1000	**10.133**	0.716	0.752	0.781	0.800	0.813	0.828
0.0700	**7.223**	0.685	0.733	0.766	0.786	0.804	0.817
0.0500	**5.066**	0.648	0.709	0.750	0.773	0.791	0.805
0.0300	**3.040**	0.569	0.671	0.725	0.755	0.780	0.795
0.0200	**2.027**	**0.450**	0.595	0.698	0.727	0.759	0.777
0.0150	**1.520**	**0.333**	**0.543**	0.667	0.715	0.747	0.773
0.0100	**1.013**	**0.225**	**0.407**	0.623	0.685	0.725	0.755
0.0070	**0.722**	**0.158**	**0.286**	**0.505**	0.625	0.700	0.739
0.0050	**0.507**	**0.120**	**0.194**	**0.384**	**0.547**	0.654	0.714
0.0040	**0.405**	**0.103**	**0.154**	**0.291**	**0.490**	0.624	0.704
0.0030	**0.304**	**0.089**	**0.127**	**0.207**	**0.349**	**0.549**	0.665
0.0020	**0.203**	**0.070**	**0.094**	**0.145**	**0.332**	**0.361**	**0.535**
0.0015	**0.152**	**0.064**	**0.081**	**0.107**	**0.160**	**0.237**	**0.416**
0.0010	**0.101**	**0.051**	**0.064**	**0.088**	**0.142**	**0.146**	**0.261**
0.0008	**0.081**	**0.047**	–	**0.082**	–	**0.133**	**0.197**

1 atm = 101.325 Pa.

Table 2
P–T–C data for H absorption in the epitaxial *bcc* V (001) thin film of thickness 50 nm read from Fig. 2 in Ref. [1]. Bold letters refer to the compositions with H/V lower than 0.55. Shaded data points ($0.675 < x < 0.775$) in the intermediate H/V range were excluded from the analysis.

$p(H_2)$		H/V						
(atm)	**(Pa)**	513 K	498 K	483 K	473 K	463 K	453 K	443 K
1.0000	**101.325**	0.823	0.845	0.862	0.874	0.883	0.886	0.894
0.5000	**50.663**	0.800	0.814	0.836	0.847	0.852	0.859	0.869
0.3000	**30.398**	0.782	0.803	0.823	0.840	0.844	0.848	0.859
0.2000	**20.265**	0.759	0.781	0.806	0.823	0.826	0.831	0.843
0.1000	**10.133**	0.727	0.758	0.797	0.805	0.810	0.812	0.825
0.0700	**7.223**	0.708	0.741	0.772	0.793	0.800	0.804	0.817
0.0500	**5.066**	0.673	0.722	0.759	0.784	0.789	0.794	0.806
0.0200	**2.027**	**0.500**	0.626	0.706	0.750	0.754	0.765	0.783
0.0150	**1.520**	**0.357**	0.575	0.690	0.737	0.745	0.758	0.780
0.0100	**1.013**	**0.223**	**0.445**	0.641	0.713	0.721	0.740	0.769
0.0070	**0.722**	**0.165**	**0.278**	0.557	0.689	0.698	0.726	0.765
0.0050	**0.507**	**0.130**	**0.200**	**0.406**	0.638	0.664	0.706	0.756
0.0040	**0.405**	**0.115**	**0.165**	**0.308**	0.596	0.640	0.693	0.750
0.0030	**0.304**	**0.104**	**0.135**	**0.175**	**0.361**	0.582	0.665	0.739
0.0020	**0.203**	**0.082**	**0.104**	**0.137**	**0.199**	**0.320**	0.564	0.695
0.0015	**0.152**	**0.073**	**0.092**	**0.118**	**0.135**	**0.247**	**0.497**	0.669
0.0010	**0.101**	**0.057**	**0.076**	**0.098**	**0.112**	**0.162**	**0.281**	0.559
0.0008	**0.081**	**0.055**	**0.071**	**0.089**	–	**0.187**	**0.220**	**0.400**
0.0006	**0.061**	**0.049**	**0.064**	**0.076**	–	**0.124**	**0.169**	**0.294**
0.0004	**0.041**	**0.040**	–	–	–	**0.100**	**0.130**	**0.165**
0.0003	**0.030**	**0.035**	–	–	–	**0.095**	**0.111**	**0.157**

1 atm = 101.325 Pa.

However, as consistently practiced in the earlier statistical thermodynamic analyses for extensive range of non-stoichiometric interstitial solutions [6–10,13–16], change of E(X–X) within a given crystalline phase under consideration is appreciated as representing inadequate modelling and linear A vs. x isotherm must be derived when realistic choice of θ is made. Accepting this criterion, H absorptions in the range $x < 0.75$ and that in the range $x > 0.75$ were decided to be analysed separately considering that the mode of H distribution in the epitaxial *bcc* V (001) thin film changed at around $x = 0.75$.

Hjörvarsson and co-workers [1–3] claimed that no crystalline deterioration was detected for the epitaxial *bcc* V (001) thin film during H uptake to x up to 0.9. Unlike for non-constrained bulk V specimen, certain degree of lattice restraining is inevitable for the epitaxial *bcc* V (001) thin film deposited over non-H absorbing MgO substrate and thence we cannot rule out the possibility that certain extent of variation of E(H–H) with x took place for VH_x without being

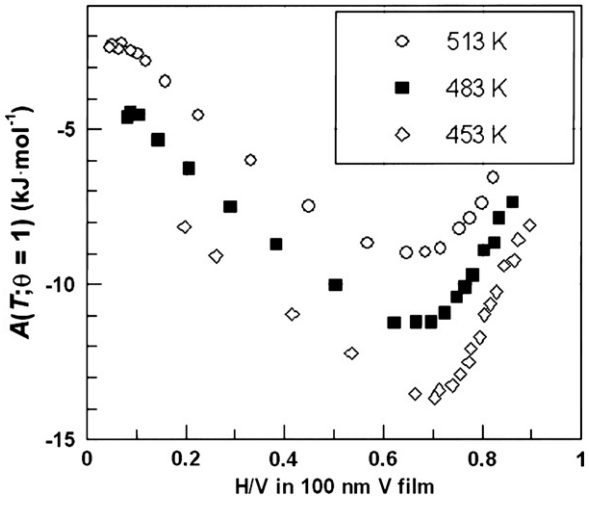

Fig. 2. Representative A vs. x isotherms prepared from the *P–T–C* relationships for the 100 nm thick epitaxial *bcc* V (001) thin film (see Table 1) [1] with a tentative choice of $\theta = 1$.

Table 3
Statistical thermodynamic analysis results for the *bcc* epitaxial VH_x (001) thin films in the range of $x<0.75$.

T (K)	513	498	483	473	463	453	443
$D(H_2)/2-RT\cdot C(T)$[a] (kJ mol^{-1})	239.865	238.485	237.105	236.185	235.265	234.345	233.425
$A(VH_x)$ 50 nm (kJ mol^{-1})	−2.651	−3.475	−3.973	−3.936	−5.356	−6.054	−5.741
	−18.287x	−17.605x	−18.717x	−20.648x	−18.692x	−18.173x	−20.359x
$K(VH_x)$ 50 nm (kJ mol^{-1})				−220.240			
				−0.0433T			
$A(VH_x)$ 100 nm (kJ mol^{-1})	−2.357	−3.094	−4.604	−5.217	−5.148	−5.588	–
	−17.684 x	−18.300 x	−19.733 x	−16.994 x	−18.586 x	−18.870 x	
$K(VH_x)$ 100 nm (kJ mol^{-1})				−224.169			–
				−0.0355T			
$K(VH_x)$ bulk[b] (kJ mol^{-1})	827 K	←		−223.518	→		518.6 K
				−0.0648T			

[a] Values for $[D(H_2)/2\text{-}RT\cdot C(T)]$ at respective T were enumerated by using empirical equation $D(H_2)/2-RT\cdot C(T) = 192.669-0.092T(\text{kJ mol}^{-1})$ derived by the values listed in Table 1 in Ref. [15] as a function of T with 100 K interval. The validity range of this expression is for T between 300 K and 1500 K.

[b] Expression for $K(VH_x)$ for the bulk VH_x was presented earlier [7,9] as $K(VH_x) = 223.604-0.0647T(\text{kJ mol}^{-1})$ but it was with a trivial calculation mistake (correct value of $T=562.9$ K was erroneously input as $T=569.9$ K in the earlier least-mean-squares calculation over T range between 827 K and 518.6 K using the P–T–C data reported by Veleckis and Edwards [5]). This error is corrected in this table.

subjected to phase change in the epitaxial *bcc* V (001) lattice unlike in the non-constrained bulk V specimen. This aspect shall be reviewed later in the text.

In the following, statistical thermodynamic analysis shall be commenced for the epitaxial *bcc* VH_x (001) thin films in the range of x lower than 0.75.

5. Analysis for the epitaxial VH_x (001) thin film in the range of x lower than 0.75

Taking into account that the H absorption enhancement in the epitaxial *bcc* V (001) thin film compared with that in the bulk V specimen as represented in Fig. 1 and also noting that kink in the A vs. x isotherm for the epitaxial *bcc* V (001) thin film emerged around $x=0.7$ in the test plots in Fig. 2 prepared with provisional choice of $\theta=1$, we decided to analyse the P–T–C relationships for the epitaxial *bcc* VH_x for the range of $x<0.75$ and those for the range $x>0.75$ separately.

First, analysis is made for $x<0.75$ with the choice of $\theta=0.75$. The results of the analysis are summarised in Table 3. In the present analysis, the values for $[D(H_2)/2-RT\cdot C(T)]$ were enumerated using an empirical equation

$$D(H_2)/2-RT\cdot C(T) = 192.669-0.092T(\text{kJ mol}^{-1}) \quad (6)$$

which is valid over T range between 300 K and 1500 K.

It is noticed in Table 3 that Q value of the 100 nm thick VH_x (001) film was −224.2 kJ mol^{-1} which was comparable to that of −223.5 kJ mol^{-1} in bulk VH_x [7,9] while that for the 50 nm thick VH_x (001) film was −220.2 kJ mol^{-1} which deviated towards the less negative side from −223.5 kJ mol^{-1}. The estimated values for βE(H–H) for these thin films as well as those for the bulk VH_x [11] are plotted as a function of T in Fig. 3. The values for βE(H–H) in the thin films scattered between −17 kJ mol^{-1} and −21 kJ mol^{-1} over T range from 443 K to 513 K while those for bulk VH_x between −21 kJ mol^{-1} and −26 kJ mol^{-1} over T range between 518.6 K and 827 K. As such, in terms of neither E(H–V) (represented by Q) nor E (H–H), the difference between the thin film in the range of x smaller than 0.75 and the bulk VH_x in the range of x smaller than 0.55 was not very significant. On the other hand, R ln f_H for the 100 nm film dropped down to 35.5 J K^{-1} mol^{-1} from that 64.8 J K^{-1} mol^{-1} of the bulk VH_x while that for the 50 nm film took the intermediate value 43.3 J K^{-1} mol^{-1}. The term R ln f_H is considered to represent the entropy term excluding the contribution from the atomic configuration. As such, the enhanced solubility of H in the epitaxial *bcc* V (001) thin film might be the consequence of modified electronic state of *bcc* V lattice around H atoms which also affected θ to increase to 0.75 in the thin films from 0.55 in the bulk VH_x.

The P–T–C data for H solubility in the epitaxial *bcc* V (001) thin films were made available only at two thickness levels, 50 nm and 100 nm. Thence it is felt too speculative to derive definitive quantitative conclusion from the present statistical thermodynamic analysis. It would be of interest to analyse the similar P–T–C data obtained for epitaxial *bcc* VH_x thin film of varying thickness up to 500 nm to derive clearer conclusion concerning the threshold film thickness distinguishing the film and the bulk states for H absorption performance through graphically visualised variation patterns of representative statistical thermodynamic parameters, Q and R ln f_H, with respect to the film thickness.

In the following, analysis is made in the range $x>0.75$ for the epitaxial *bcc* VH_x (001) thin films.

6. Analysis for the epitaxial VH_x (001) thin film in the range of x higher than 0.75

As seen in Fig. 2, slope of the A vs. x isotherms for the epitaxial *bcc* VH_x (001) thin film changed at around 0.7. Thus, P–T–C relationships for the VH_x thin film in the range of $x>0.75$ were analysed separately from those in the range of $x<0.75$.

Two distinguishable types of H distribution models in the interstitial sites in the VH_x thin film in the range of $x>0.75$ are reviewed. One is the model in which H atoms are distributed randomly over available interstitial sites whose number is defined with $\theta=1$. In another H distribution model, H atoms up to composition $x=0.75$ are assumed to

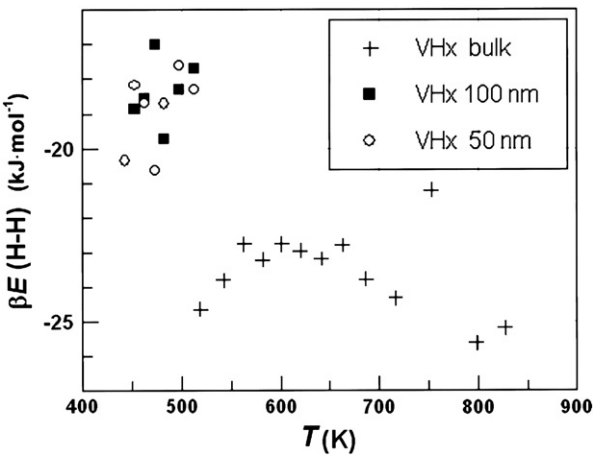

Fig. 3. Estimated values of βE(H–H) for the epitaxial *bcc* V (001) thin films in $x<0.75$ plotted as a function of T. As the references, those in the bulk V are also plotted being reproduced from Ref. [10].

occupy the interstitial sites with certain geometrical order and the H atoms exceeding $x=0.75$ are distributed randomly in the rest of the interstitial sites up to $x=1.0$.

In the latter model, number W of configuration of H atoms in the VH_x lattice in the composition range x exceeding 0.75 is represented by [7–9]

$$W = (\theta n_V - \theta' n_V)! / [(n_H - \theta' n_V)! \cdot (\theta n_V - n_H)!] \quad (7)$$

and this would lead to modification for the fundamental formula (1)

$$A'(x,T) \equiv RT \ln\{[p(H_2)]^{1/2} \cdot (\theta - x) / (x - \theta')\} = g + \beta x E(H\text{–}H) \quad (8)$$

with $\theta=1$ and $\theta'=0.75$.

This line of statistical thermodynamic modelling characterising the interstitial site occupation by H atoms with θ and θ' was employed for analysing H absorption in intermetallics like $LnM_nH_{(n+1)x}$ where Ln refers to lanthanide such as Dy, Er or Tm and M refers to Co or Fe [7–9]. For example, $DyCo_3H_{4x}$ in the range of x between 0.25 and 0.5 was analysed with $\theta=0.475$ and $\theta'=0.25$ and that in the range of x between 0.75 and 1.1 with $\theta=1.05$ and $\theta'=0.725$ determined by trial-and-error method to yield linear isothermal $A'(x,T)$ vs. x relationships (see Fig. 7 in Ref. [9]). In short, θ is considered to represent the higher solubility limit of H in the VH_x thin film in the concerned range of H solubility while θ' the lower solubility limit.

6.1. Analysis with $\theta=1$ and $\theta'=0$

With this simplifying random H distribution model over entire available interstitial sites with a number represented by $\theta=1$, βE(H–H) was estimated to be positive (repulsive) falling in the range between 40 kJ mol^{-1} and 25 kJ mol^{-1} as plotted in Fig. 4 in contrast to negative (attractive) βE(H–H) in the range of $x<0.75$ (Fig. 3). Derived K vs. T data are plotted in Fig. 5 which yield the least-mean-squares relationships with considerable extent of deviation from linearity unlike in the case with the epitaxial *bcc* VH_x (001) film in the range of $x<0.75$ as reviewed above in the text or for other general cases of analysis for interstitial elements in bulk specimens [6–10,13–16]

$$K(100\,\text{nm};\theta=1;T) = -342.155 + 0.1442T\,(\text{kJ mol}^{-1}) \quad (9)$$

$$K(50\,\text{nm};\theta=1;T) = -287.352 + 0.0286T\,(\text{kJ mol}^{-1}). \quad (10)$$

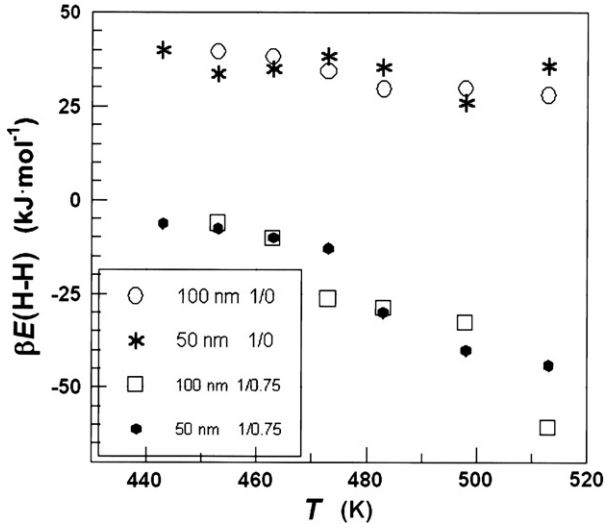

Fig. 4. Estimated values of βE(H–H) for the epitaxial *bcc* V (001) thin films in $x>0.75$ plotted as a function of T; with simplifying model defined with $\theta=1.0$ and $\theta'=0$ (1/0) and with model defined with $\theta=1$ and $\theta'=0.75$ (1/0.75).

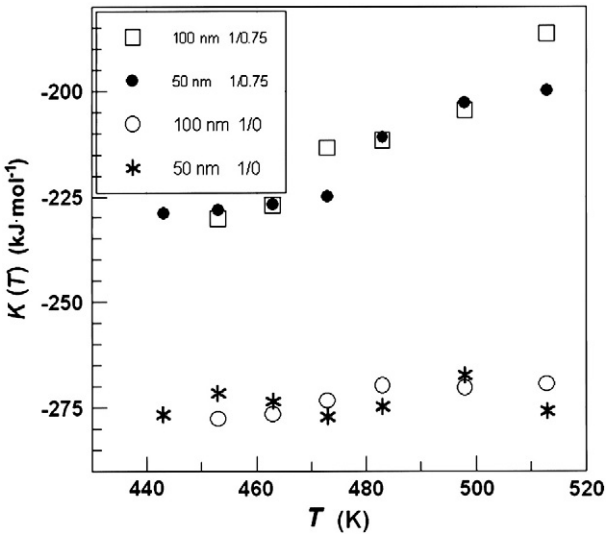

Fig. 5. K vs. T relationships estimated for the epitaxial *bcc* V (001) thin films in $x>0.75$; with simplifying model defined with $\theta=1.0$ and $\theta'=0$ (1/0) and with model defined with $\theta=1$ and $\theta'=0.75$ (1/0.75).

Comparing these with the K vs. T relationships for the thin films in the range of $x<0.75$ given in Table 3, it is understood that the estimated Q values in the range of $x>0.75$ by this model were considerably more negative being in accordance with the enhanced H solubility in the thin film while E(H–H) turned repulsive (Fig. 4).

It does not seem very rational that Q for the 100 nm film (-342.2 kJ mol^{-1}; Eq. (10)) is more negative than that for the 50 nm film (-287.4 kJ mol^{-1}; Eq. (11)) deviating more from the corresponding value for the bulk (-223.5 kJ mol^{-1}; Table 3 [7,9]) than that for the 50 nm film.

Further, $R \ln f_H$ values for the epitaxial *bcc* VH_x thin films in $x>0.75$ turn to be negative (Eqs. (10) and (11)) from positive for those in $x<0.75$ (Table 3). This evidence as well as the change of E(H–H) from attractive in the range $x<0.75$ to repulsive in the range of $x>0.75$ seems to be a bit strange to accept straightforwardly noting that no crystal lattice disintegration of the thin film was induced after the H absorption experiment up to $x=0.9$ [1] because such drastic changes in E(H–H) with the composition x are anticipated to lead to phase transformation and resultant lattice disintegration.

Thus, these evaluation results as a whole appeared to suggest that the model with $\theta=1$ and $\theta'=0$ for the epitaxial *bcc* VH_x (001) thin film in the range of $x>0.75$ might be non-realistic, especially in view of drastic change in E(H–H). At any rate, we cannot rule out the possibility that such anomaly represents the inherent nature for H absorption in the thin film specimen under biaxially constrained state.

To look into the aspect of modelling for the epitaxial *bcc* VH_x (001) thin film in the range of $x>0.75$, we review another optional model in the subsequent section.

6.2. Analysis with $\theta=1$ and $\theta'=0.75$

With this H atom distribution model, the interstitial sites up to composition corresponding to $VH_{0.75}$ are preferentially occupied by H atoms with certain type of geometrical order and then the H atoms exceeding the composition $x=0.75$ are distributed randomly over the rest of the interstitial sites up to $x=1.0$.

As pointed out above in the text, fundamental equation for the analysis with this model is modified to be Eq. (8) from Eq. (1) derived for the simple random H atom distribution model because the site occupation mode by this model is represented by Eq. (8).

With this model, estimated values of βE(H–H) fell in the negative range as plotted in Fig. 4 showing certain extent of variation with T. On

the other hand, K vs. T relationship derived from this model for either thickness, 100 nm or 50 nm, deviated away from linearity as seen in Fig. 5 and thence it was felt inadequate to evaluate Q and $R \ln f_H$ from the K vs. T plots as reproduced in Fig. 5 although K vs. T relationships are formally represented by

$$K(100\,\mathrm{nm};\theta = 1,\theta' = 0.75;T) = -574.639 + 0.6979T\,(\mathrm{kJ\,mol^{-1}}) \quad (11)$$

$$K(50\,\mathrm{nm};\theta = 1,\theta' = 0.75;T) = -447.915 + 0.4850T\,(\mathrm{kJ\,mol^{-1}}). \quad (12)$$

The estimation results did not change much with the other alternative combinations of (θ, $\theta' = 0.75$) like ($\theta = 1.5$, $\theta' = 0.75$) and ($\theta = 3$, $\theta' = 0.75$).

That is, the model with $\theta' = 0.75$ at any choice of θ value would yield considerably less negative values of Q for the epitaxial *bcc* VH_x (001) thin films in the range of $x > 0.75$ compared with those estimated for the epitaxial *bcc* VH_x (001) thin films in the range of $x < 0.75$ when estimation for Q is made from K vs. T relationships evaluated formally by the least-mean-squares method.

When we closely look at the K vs. T plots in Fig. 5 for the ($\theta = 1/\theta' = 0.75$) model, we notice that the K vs. T relationships in the range of T lower than 470 K became virtually independent of T (in other words, $R \ln f_H = 0$ yielding T-independent Q value around $-230\,\mathrm{kJ\,mol^{-1}}$) whereas K tended to increase linearly with T in the range of T higher than 470 K. On the other hand, it is seen in Fig. 4 that variation of βE(H–H) with T became less significant in the range of T lower than 470 K yielding virtually T-independent βE(H–H) around $-10\,\mathrm{kJ\,mol^{-1}}$.

7. Concluding remarks

Equilibrium P–T–C relationships reported for the epitaxial *bcc* V (001) thin films by Andersson et al. [1] were analysed in terms of statistical thermodynamics in which E(H–H) is assumed *a priori* to hold constant over a homogeneity composition range at any given T. With this *a priori* assumption, linear K vs. T relationships were derived for extensive range of bulk interstitial non-stoichiometric compounds and, with reference to Eq. (2), values of Q and $R \ln f_H$, were evaluated [6–10,13–16]. However, for the epitaxial *bcc* VH_x (001) thin films constrained over non-H absorbing MgO substrate, such simplifying statistical model developed for bulk specimen was demonstrated to be not straightforwardly applicable.

In contrast to the bulk *bcc* VH_x in which the primary solid solubility limit of H was no higher than $x = 0.55$, H solubility in the epitaxial *bcc* VH_x (001) thin film was extended to H/V ratio close to 1.0. The range of $x < 0.75$ in the epitaxial *bcc* VH_x (001) thin films with thickness, 100 nm and 50 nm, was analysed by the statistical model with $\theta = 0.75$ and the estimated values of Q were comparable to that in the bulk VH_x analysed with $\theta = 0.55$ whereas $R \ln f_H$ in the epitaxial *bcc* VH_x (001) thin film was different from that in the bulk VH_x [6–9]. Thus, the extended solubility of H in the epitaxial *bcc* VH_x (001) thin film was concluded to be interpreted in terms of the modified electronic state affecting largely the $R \ln f_H$ term in the thin film without altering much the nearest neighbour H–V interaction energy (the Q term).

On the other hand, H solubility in the epitaxial *bcc* VH_x (001) thin film in the range of x higher than 0.75, especially in the range of T lower than 470 K, seemed to be appreciated on the basis of statistical model different from that for the bulk VH_x.

There was no significant difference in the P–T–C relationships between the 100 nm and the 50 nm films of the epitaxial *bcc* VH_x (Fig. 1; Tables 1 and 2) and correspondingly the estimated values for the statistical thermodynamic parameters including Q, $R \ln f_H$ and βE (H–H) for the 100 nm film and those for the 50 nm film were comparable to each other (Table 3; Figs. 3–5).

Hjörvarsson and co-workers [1–3] observed that the enhanced H solubility in epitaxial V (001) thin film under biaxially constraining stress state was associated with certain extent of tetragonal distortion of the *bcc* V lattice. Tetragonal distortion of CaF_2 type lattice of dihydride of Zr, ZrH_x, in non-constrained bulk state at around $x \approx 1.72$ was earlier reviewed by Shohoji and Marcelo [18] in terms of statistical thermodynamics. As exemplified for Zr dihydride phase, in some metal hydride MH_x, inherent tetragonal distortion of the M lattice might be induced by H absorption without externally forced lattice constraining like in the present VH_x thin film under constrained biaxial stress state.

At any rate, enhanced H solubility in the epitaxial V (001) thin film under consideration must be somehow related to the tetragonal distortion of the *bcc* V lattice promoted by the biaxial constraining at the basal plane of the film adhered to non-H absorbing MgO.

It might be of pragmatic interest to determine experimentally the P–T–C relationships for the similar epitaxial *bcc* VH_x (001) thin films of thickness range between 500 nm and 10 μm and analyse them in terms of statistical thermodynamics to evaluate the border for the H absorption performance between the constrained thin film state and the non-constrained bulk state.

Appendix A. List of symbols

$A(x,T)$	$\equiv RT \ln \{[p(H_2)]^{1/2}\cdot(\theta - x)/x\}$ ($\mathrm{kJ\,mol^{-1}}$); calculated from experimentally determined values of $p(H_2)$, T and x for specified value of θ using Eq. (1)
$C(T)$	defined by Eq. (3) to represent contributions of translational, rotational and vibrational motions of H_2 molecule
$D(H_2)$	dissociation energy of H_2 molecule per mole ($\mathrm{kJ\,mol^{-1}}$)
E	lattice energy ($\mathrm{kJ\,mol^{-1}}$)
$E(i-j)$	nearest neighbour pairwise interaction energy between i and j atoms in VH_x lattice
$f_H(T)$	partition function of H in VH_x lattice at T
g	parameter determined as the intercept of the $A(T)$ vs. x plot at $x = 0$ using Eq. (1)
$g(\nu)$	distribution function
h	Planck constant
k	Boltzmann constant
K	parameter calculated from g using Eq. (2)
m_H	mass of H atom
n_H	number of H atoms in the VH_x lattice
n_V	number of V atoms in the VH_x lattice
$p(H_2)$	partial pressure of ideal H_2 gas molecule (atm)
P–T–C	pressure–temperature–composition
Q	degree of stabilisation of H atom in VH_x lattice with reference to isolated H atom in vacuum
R	universal gas constant ($= 0.0083145\,\mathrm{kJ\,mol^{-1}\,K^{-1}}$)
T	absolute temperature (K)
x	atom fraction of H against V in VH_x
β	geometrical factor determined from crystal structure consideration
θ	number of available interstitial sites for occupation by H atom per metal atom in VH_x
Θ_r	characteristic temperature for rotation of H_2 molecule ($= 85.4$ K)
Θ_v	characteristic temperature for vibration of H_2 molecule ($= 6100$ K)
$\mu(H)^c$	chemical potential of H atom in the condensed phase VH_x
$\mu(H)^g$	chemical potential of H atom in the ideal diatomic H_2 gas molecule
ν	vibrational frequency of H atom in VH_x lattice
ρ	nuclear spin weight ($= 2$ for H while 3 for D)
υ_0	statistical weight of tightly bound electrons around H in VH_x lattice
υ_0^*	statistical weight of electrons in H_2 molecule in normal state ($= 1$)

References

[1] G. Andersson, K. Aits, B. Hjörvarsson, J. Alloys Compd. 334 (2002) 14.
[2] S. Olsson, B. Hjörvarsson, Phys. Rev. B 71 (2005) 035414.
[3] J. Bloch, B. Hjörvarsson, S. Olsson, R. Brukas, Phys. Rev. B 75 (2007) 165418.
[4] J. Öhrmalm, G. Andersson, J. Birch, B. Hjörvarsson, J. Alloys Compd. 285 (1999) 21.
[5] E. Veleckis, R.K. Edwards, J. Phys. Chem. 73 (1969) 683.
[6] N. Shohoji, J. Less-Common Met. 90 (1983) L27.
[7] N. Shohoji, J. Less-Common Met. 102 (1984) 53.
[8] N. Shohoji, J. Less-Common Met. 114 (1985) 249.
[9] N. Shohoji, Surf. Coat. Technol. 28 (1986) 365.
[10] N. Shohoji, J. Mater. Sci. Lett. 5 (1986) 522.
[11] R.H. Fowler, E.A. Guggenheim, Statistical Thermodynamics, Cambridge University Press, 1949.
[12] R. Speiser, W. Spretnak, Trans. Amer. Soc. Met. 47 (1955) 493.
[13] N. Shohoji, Z. Metallkde. 76 (1985) 192.
[14] N. Shohoji, J. Mater. Prod. Technol., SPM1 Vol. 1 (2001) p.41 Inderscience Enterprises Ltd., Geneva.
[15] N. Shohoji, N. Shohoji, Mater. Trans., JIM 42 (2001) 2225.
[16] N. Shohoji, S. Figueiredo Marques, Internat. J. Mater. Res. 99 (2008) 245.
[17] D.R. Stull, H. Prophet, G.C. Sinke (Eds.), JANAF Thermochemical Tables, Dow Chemical Co., Midland, MI, 1965.
[18] N. Shohoji, T. Marcelo, J. Mater. Sci. Lett. 6 (1987) 1251.